

Nanocrystals of Coordination Polymers

Takashi Uemura and Susumu Kitagawa*

(Received October 1, 2004; CL-048014)

Abstract

This review highlights the recent progress of nanosize crystals based on coordination polymers (CP). Development of synthetic method with controllable size and shape in nanometer regime as well as understanding of size and surface effects of the CP nanocrystals is urgently requisite on behalf of future application of them to new organic-inorganic hybrid nanomaterials.

Introduction

With the growing interest in creating advanced materials using nanoscale building blocks, nanosize crystals based on inorganic materials such as metals, metal oxides, metal sulfides, and carbons have been developed extensively during the past decade.¹ On the basis of the study on those nanocrystals, many interesting optical, electronic, and chemical properties which are crystal size- and shape-dependent have been discovered. For example, 0-dimensional nanocrystals, which are recognized as “nanoparticles,” have attracted much attention because of quantization of electronic states, nonlinear optical properties, large-surfaces, catalysts, assembling with high regularity at nanometer scale, molecule carrier, and so on.^{1a-c} One-dimensional crystals with nanometer scale diameters and high aspect ratios such as nanowires, nanorods, and nanotubes, are currently

the focus of interest for their potential applications to key components of electronics, photonics, mechanics, conductors, fluidics, and sensing in nanodevices.^{1d,e}

On the other hand, nanosize materials (nanoparticles, nanowires, and nanotubes) composed of pure organic components are of intense interest owing to the diversity of the structures and weak intermolecular interaction forces of the van der Waals type, which are fundamentally different from those of inorganic metals and semiconductors.² Especially nanomaterials based on organic polymer latex particles and their colloidal crystals are extensively studied and can be used as nanotemplates and photonic band gap materials.^{2c-g} An equally intense effort has aimed to construct simpler synthetic nanotubes, inspired by the remarkable functions of tubular structures in biology. Studies on hollow cylindrical nanotubes comprised of cyclic peptides, amphiphilic saccharides, and cyclodextrins are the center of attraction.^{2h-j}

Coordination polymers (CP) are metal-ligand compounds that extend infinitely via self-assembling process (Figure 1).³ CP with infinite structures have been studied intensively in the last decade. In particular, structure study and architecture control through single-crystal X-ray investigations in terms of *crystal engineering* have been major work in the research area.³ Recently, many researches are embedded in the area of utilization of their functions, such as redox property, magnetism, conductivity, catalysis, luminescence, spin transitions, and porous properties.⁴ By choosing and the combination of ligands and metal ions, one

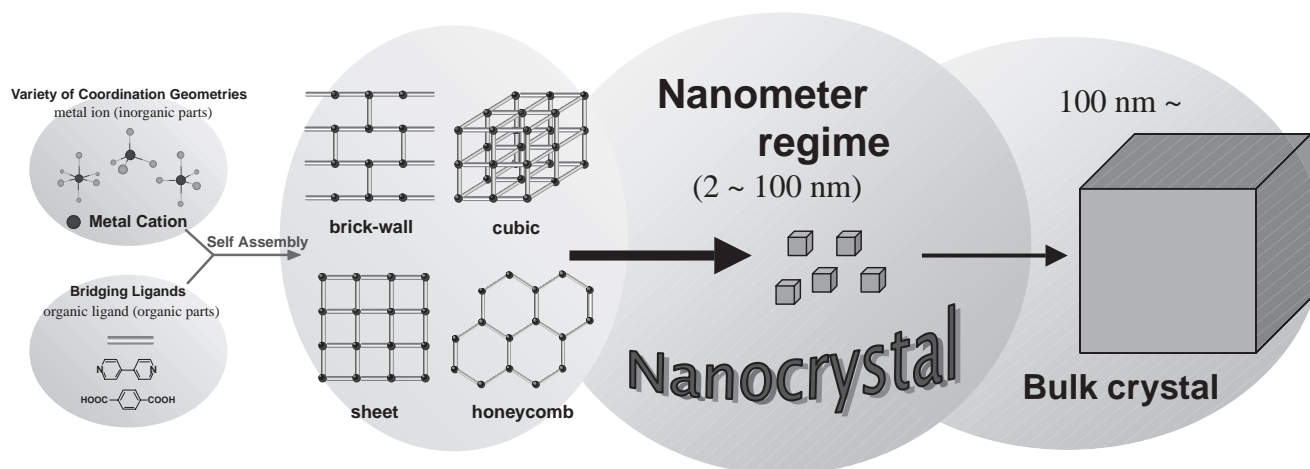


Figure 1. Schematic illustration of coordination polymer nanocrystals.

Dr. Takashi Uemura, Prof. Susumu Kitagawa,*
Department of Synthetic Chemistry and Biological Chemistry, Graduate School of Engineering, Kyoto University,
Katsura, Nishikyo-ku, Kyoto, 615-8510
E-mail: kitagawa@sbchem.kyoto-u.ac.jp

can design or tune the above chemical and physical properties and, thus, realize various applications.

However, most CP materials have taken the form of bulk crystalline solids so far, therefore, the properties of CP are usually originated from their bulk crystalline solids whose crystal sizes range from 0.1 μm to 1 mm. Construction of CP at nanometer scale⁵ would produce nanosize crystals with *finite* repeating unit structures. In this review, we define such nanosize materials (2–100 nm) as “CP nanocrystals” whose properties are different from those of bulk CP and show unexpected information about nanomaterials. Recent studies on the syntheses, characterizations and properties of the CP nanocrystals, e.g., nanoparticles, nanorods, nanowires, and nanocomposites are highlighted.

◆ Synthesis of Coordination Polymer Nanocrystals

In order to obtain the inorganic nanosize materials based on metals and carbons, a number of chemical and physical methods have been developed so far.⁶ Classification of the methods is summarized in Figure 2. On comparison between top-down and bottom-up techniques, the latter has been developed extensively in the last decade because the size and shape of nanomaterials can be more easily controlled. Various nanocrystals were efficiently prepared by both the vapor^{6a,b} and the solution^{6c–e} methods. Use of templates or nanospaces composed of lipids, micelles, clays, and zeolites together with the chemical vapor deposition, solution reaction, sol–gel, and electrodeposition methods is one of the most effective techniques.^{6f,g} The utilizations of crystal surface stabilizers such as ligands, surfactant, and polymers in the mild solution methods are now widely accepted by chemists because of the easy accessibility and low cost.

Usually the bulk CP materials are synthesized by mixing both solutions of metal ions and bridging ligands. Hence it is likely to employ the solution techniques to prepare the CP nanocrystals. Inspired by the inorganic nanomaterials, several attempts at synthesis of CP nanocrystals have emerged in the last

few years. The uses of ligands, surfactants, polymers, protein, silica, mesoporous alumina, and hydrothermal process in the preparations of CP have demonstrated how the crystal growths were effectively inhibited and the resultant nanocrystals were stabilized (Table 1).

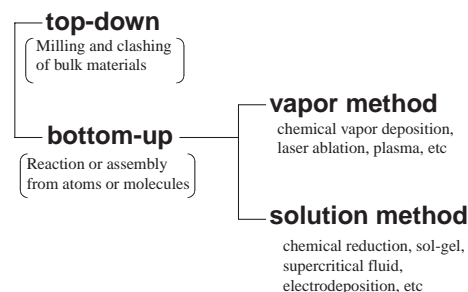


Figure 2. The classification of preparation methods of inorganic nanomaterials.

Currently the challenge to prepare the CP nanocrystals has been mainly focused on Prussian blue (PB) analogues $M_i^{m+}[M'(CN)_6]^{n-}$ (Figure 3) because the PB analogues are structurally simple (divalent and trivalent metal ions are linked with CN ligand to form cubic infinite structures), easy to prepare and characterize, and now play important roles in the field of molecular based magnets.⁷ The versatile superexchange interactions between the neighboring metal ions through the cyanide bridges afford them unique magnetic properties such as high temperature magnet, magnetic pole inversion, spin glass, and photomagnetism, depending on constituents and ratios of the metal ions.

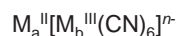
First PB-based nanoparticles (normal PB, cobalt hexacyanoferrate and cobalt pentacyanonitrosylferrate) with uniform shapes and sizes have been prepared in confined nanoscale water droplets formed from reversed microemulsion by use of anionic surfactant sodium bis(2-ethylhexyl)sulfosuccinate (Aerosol OT;

Table 1. Nanocrystals of coordination polymers

Compound	Morphology	Size/nm	Crystal growth inhibitor	Nanosize effects ^b	Reference
$\text{Fe}^{\text{II}}_i[\text{Fe}^{\text{III}}(\text{CN})_6]^{n-}$	cubic particle	12–54 ^b	reversed micelle ^d	SO, SL	8a
$\text{Co}^{\text{II}}_i[\text{Fe}^{\text{III}}(\text{CN})_6]^{n-}$	cubic particle	12–22 ^b	reversed micelle ^d	SO, SL	8b
$\text{Co}^{\text{II}}_i[\text{Fe}^{\text{III}}(\text{CN})_5\text{NO}]^{n-}$	cuboctahedral particle	27	reversed micelle ^d	SO, SL	8b
$\text{Ni}^{\text{II}}_i[\text{Cr}^{\text{III}}(\text{CN})_6]^{n-}$	sphere particles	3	reversed micelle ^{d,e}	SO, SP	9
$\text{Co}^{\text{II}}_i[\text{Fe}^{\text{III}}_f\text{Cr}^{\text{III}}_k(\text{CN})_6]^{n-}$	cubic particle	5–7	reversed micelle ^f	SO	10
$\text{Fe}^{\text{II}}_i[\text{Fe}^{\text{III}}(\text{CN})_6]^{n-}$	sphere particle	12–27 ^b	PVP	SO, SP, MD, SM, SE, FF	11a, 11b
$\text{Fe}^{\text{II}}_i[\text{Fe}^{\text{III}}(\text{CN})_6]^{n-}$	sphere particle	5–8	PDDA	SO, SE, FF	11b
$\text{Co}^{\text{II}}_i[\text{Fe}^{\text{III}}(\text{CN})_6]^{n-}$	sphere particle	8–10	silica matrix	MD, SP	12
$\text{Fe}^{\text{II}}_i[\text{Fe}^{\text{III}}(\text{CN})_6]^{n-}$	sphere particle	5	apoferritin	—	13
$\text{Fe}^{\text{II}}_i[\text{Fe}^{\text{III}}(\text{CN})_6]^{n-}$	one-dimensional wire	50 ^c	porous alumina	MD	14
porous CP ^a	sphere particles	30–45	neutral surfactant ^g	—	15
porous CP ^a	one-dimensional rod	100 ^c	porous alumina	—	15
$\text{ZnF}(\text{3-amino-1,2,4-triazole})$	one-dimensional rod	submicron ^b	solvothermal process	PN	16
$\text{Ni}(\text{NH}_3)_6\text{Cl}_2$	layered tube	20–40 ^c	PVP	—	17

^a Structures were not well determined. ^b Crystal sizes could be controlled. ^c Diameters of the one-dimensional crystals. ^d AOT as the surfactant. ^e *p*-Nitrobenzylpyridine as the crystal stabilizer. ^f Penta(ethylene glycol) mono 4-nonylphenyl ether as the surfactant and stearylamine as the crystal stabilizer. ^g Brij 30 as the surfactant. ^h SO = solubility, SL = superlattice, SP = superparamagnetism, MD = magnetic breaking temperature decrease, SM = size-dependent magnetism, SE = surface effects, FF = film-forming property, PN = precursor of nanomaterials.

Prussian Blue Analogues



($M_a = M_b = \text{Fe, Mn, Ni, Cr, Co, V etc.}$)

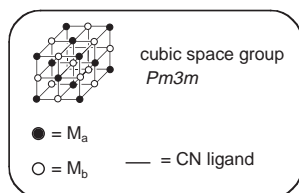


Figure 3. Chemical formula of PB analogues and their schematic illustration.

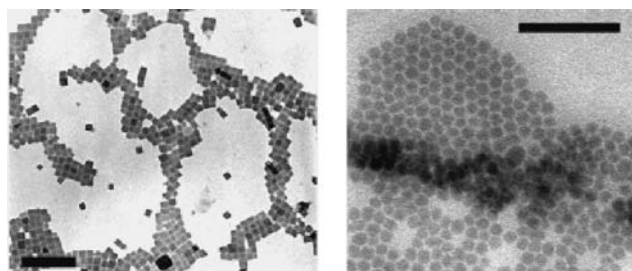


Figure 4. TEM images of cobalt hexacyanoferrate nanoparticles (left) and cobalt pentacyanonitrosyl ferrate nanoparticles (right) synthesized in AOT water-in-oil microemulsions. Scale bars = 200 nm. Reprinted with permission from Ref. 8b. Copyright 2002 American Chemical Society.

AOT) (Figure 4).⁸ The averaged size of the nanoparticles could be finely tuned by concentrations of the reactants from 12 to 54 nm.

Nanoparticles of a PB analogue such as cyanide-bridged $\text{Cr}^{\text{III}}\text{--Ni}^{\text{II}}$ have been synthesized by the same reverse micelles technique (AOT system).⁹ *p*-Nitrobenzylpyridine was used as a peripheral ligand to separate the nanoparticles from the inverted micelle medium. Similarly, different PB analogue has been transformed to the nanoparticles stabilized by stearylamine in reversed micelle composed of neutral surfactant (penta(ethylene glycol) mono 4-nonylphenyl ether).¹⁰ In this report, Co^{II} , Fe^{III} , and Cr^{III} could be incorporated in the nanoparticles with various ratios, which changes optical and magnetic properties of the nanomaterials.

Organic polymers such as poly(vinylpyrrolidone) (PVP) and poly(diallyldimethylammonium chloride) (PDPA) were employed to control the crystal size of the PB nanoparticles.¹¹ PVP has repeating amide moieties that can weakly bind to iron ions based on the coordinate interactions. It is expected that positively charged PDPA interacts with negatively charged PB colloid. The principle is based on the fact that the polymers can interact with growing PB nucleus in the site-specific way, depending on their functional groups. In the synthesis of PB nanoparticles protected by PVP, differences in experimental conditions significantly affect the size changes of the PB nanoparticles in the nanometer scale. The averaged dimensions of the PB nanoparticles were tuned from 12 to 27 nm depending on the concentrations of Fe ions and feed ratios of Fe to PVP (Figures 5a–5d). Addition of PDPA produced the PB nanoparticles with very small dimensions (5–8 nm) by the effective electrostatic interaction (Figure 5e).

The fabrication of nanocomposite material containing the photomagnetic $\text{K}_x\text{Co}_y[\text{Fe}(\text{CN})_6]$ nanoparticles in a porous silica matrix has been reported.¹² The nanocomposite material was

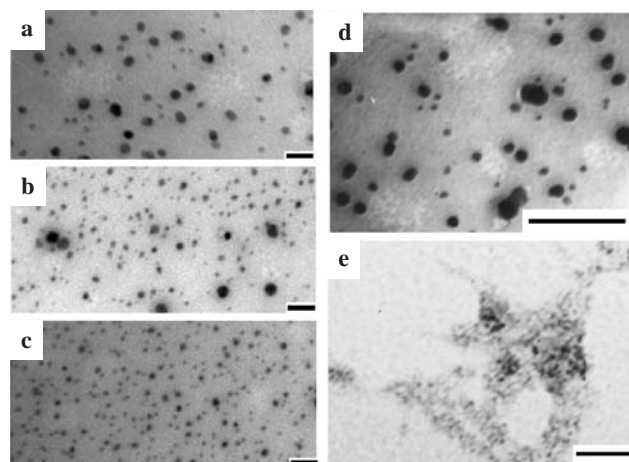


Figure 5. TEM images of PVP-protected PB nanoparticles prepared at $[\text{Fe}^{2+}] = [\text{Fe}^{3+}] = 10 \text{ mM}$, $[\text{PVP}]/[\text{Fe}^{2+}] =$ (a) 20, (b) 50, and (c) 100. (d) PVP-protected PB nanoparticles obtained at $[\text{Fe}^{2+}] = [\text{Fe}^{3+}] = 1 \text{ mM}$, $[\text{PVP}]/[\text{Fe}^{2+}] = 100$. (e) PDDA-protected PB nanoparticles at the condition of $[\text{Fe}^{2+}] = [\text{Fe}^{3+}] = 3 \text{ mM}$, $[\text{PDDA}]/[\text{Fe}^{2+}] = 100$. Scale bars in all figures = 100 nm. Reprinted with permission from Ref. 11b. Copyright 2004 American Chemical Society.

synthesized by carrying out the preparation of $\text{K}_x\text{Co}_y[\text{Fe}(\text{CN})_6]$ during sol–gel reaction in which the precipitation of the PB family were trapped by the silica matrix at nanometer stage. This material showed photomagnetic behavior similarly to the bulk compound.

A biological route for preparing PB nanoparticles has been developed.¹³ The PB nanoparticles were successfully formed in cages of protein shell (apoferritin) with a diameter of about 8 nm. The formation of the PB nanoparticles was achieved by dissociation of apoferritin into subunits with trapping $[\text{Fe}(\text{CN})_6]^{3-}$ at pH 2, followed by its reconstruction at pH 8.5 and subsequent reaction with Fe^{II} (Figure 6). The averaged diameter of the resultant bionanoparticles observed by TEM was about 5 nm, consistent with the cage size of apoferritin.

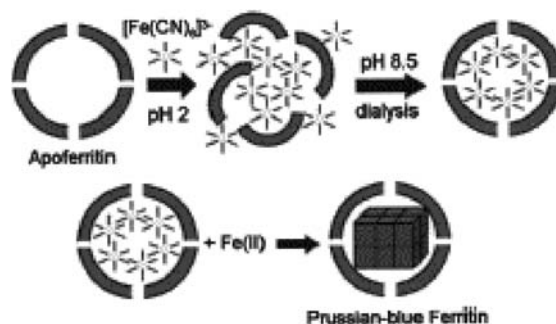


Figure 6. Formation of PB nanoparticles in the dissociation–reconstruction process of apoferritin. Reprinted with permission from Ref. 13. Copyright 2003 American Chemical Society.

One-dimensional PB nanowire arrays have been prepared by an electrodeposition method with a porous aluminum oxide film.¹⁴ The PB nanowires were deposited in the porous aluminum oxide and were separated by dissolving the alumina template with a strong acid. The TEM and selected area electron dif-

fraction images of the isolated product showed PB nanowire materials with diameters of about 50 nm (Figure 7; left), which was consistent with the pore size of the alumina.

Besides the nanocrystals of PB analogues reviewed above, we note that there are various and many other CP components available in the nanocrystal forms. The key aspects of strategy for unique CP nanocrystals are utilizations of the organic ligands. With diverse structures and designable functions, the organic ligands play important rolls in the attractive properties of CP. If the ligand structure as well as the crystal size of CP can be systematically controlled, it may become possible that the both factors cooperatively tune the CP properties.

In fact, preparation of the CP nanocrystals that are different from the PB derivatives have not been attained yet. A suggestive experiment for decreasing the crystal size of porous CP to nanometer size (30–100 nm) by use of a nonionic surfactant (Brij 30) and anodic alumina membrane was reported,¹⁵ even though the crystal structure of the products were speculated ones.

Tubular nanostructures composed of CP would provide different functions from those of carbon nanotubes. Recently the CP crystals $[\text{ZnF}(\text{AmTAZ})]\cdot\text{solvents}$ (AmTAZ = 3-amino-1,2,4-triazole) with hollow tubular structure have been synthesized by solvothermal process, where the crystal size was ranged from millimeters to submicrometer depending on the reaction condition.¹⁶ Smaller crystals were obtained when higher reagent concentrations and shorter reaction time are utilized in the reaction.

Decomposition of $[\text{Ni}(\text{NH}_2\text{NH}_2)_2]\text{Cl}_2$ precursor in the solution phase produced the layer-rolled $[\text{Ni}(\text{NH}_3)_6]\text{Cl}_2$ nanotubes as a major product (unfortunately this material was not composed of organic ligands and was contaminated with undecomposed $[\text{Ni}(\text{NH}_2\text{NH}_2)_2]\text{Cl}_2$ and Ni particles) and the Ni complex nanotubes were stabilized by PVP.¹⁷ The TEM images of the obtained materials showed that nanotubes have 4–8 layers rolling structure with diameters ranging from 20 to 40 nm and length up to 2 μm (Figure 7; right). The advantage of this method compared with the synthesis of inorganic nanotube materials is mild and simple solution approach.

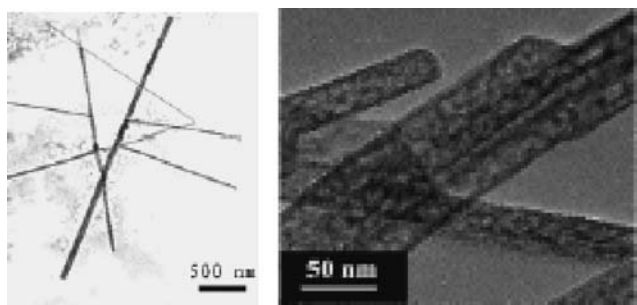


Figure 7. TEM images of PB nanowires (left) and $[\text{Ni}(\text{NH}_3)_6]\text{Cl}_2$ nanotubes (right). Reprinted with permission from Refs. 14 and 16. Copyright 2002 and 2004 American Chemical Society.

◆ Nanosize Effects of Coordination Polymer Nanocrystals

Of special interest in the CP nanocrystals is search for their nanosize effects. The expected nanosize effects of the low-dimensional CP nanocrystals are as follows (Figure 8). The first one is an enhanced solubility. Generally, little is known about

the metal–ligand species which may perform in solutions before they are assembled onto the bulk CP. CP nanocrystals, especially nanoparticles and some nanorods, may be dispersed in solvents and play a key role for understanding the chemistry of CP in “solution” state. The second advantage is isolation of the unique electron and spin states of CP in nanometer scale. This will afford new sciences for quantum, size-dependent, and surface effects of CP, giving novel chemical and physical functions. The third is improvement in their processability. The bulk CP without crystal size and morphology control have limited their processability into films, fibers, and desired shapes. The assembly of nanocrystals into materials with higher-order architecture is collectively termed *nanotectonics* and is now studied extensively.¹⁸ The synthesis of hierarchically ordered CP is of potential interest in various fields including catalysis, separations, and materials chemistry.

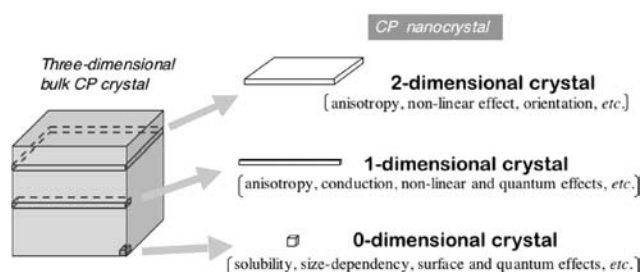


Figure 8. Nanosize effects expected for the low-dimensional CP nanocrystals.

In respect of solubility, many CP nanocrystals with small crystal sizes have been found to be soluble in many solvents because of the effective assistance of the crystal-protecting agents such as long alkyl ligands^{8–10} and organic polymers.¹¹ For example, the PB analogue nanoparticles protected by those organic stabilizers are soluble in many organic solvents, although bulk PB is insoluble in any organic media. Owing to the high solubility, the nanoparticles revealed new properties such as solvent-dependent absorption and enhanced processabilities, which will be mentioned below.

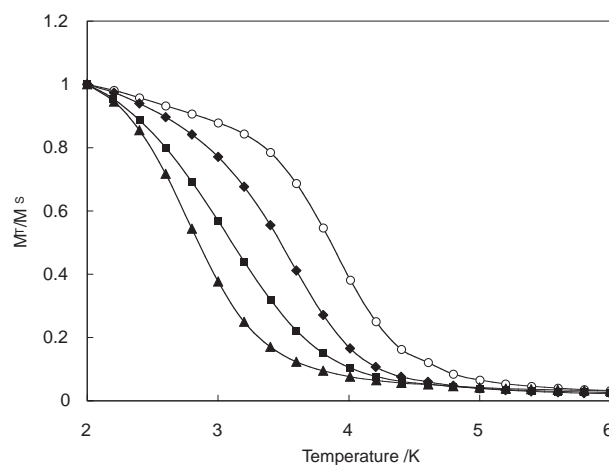


Figure 9. Size-dependent magnetization curves of PVP-protected PB nanoparticles (○: bulk PB, ◆: 27 nm, ■: 16 nm, ▲: 12 nm).

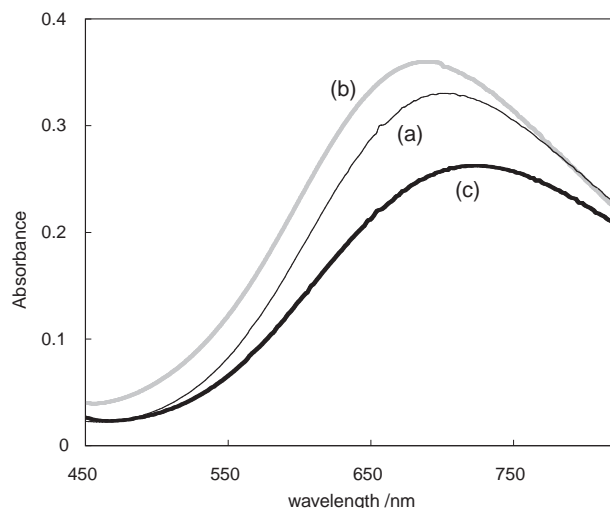


Figure 10. Absorption spectra of (a) bulk PB, (b) PVP-protected PB nanoparticles (12 nm), and (c) PDDA-protected PB nanoparticles in water.

Unprecedented size-dependent and surface effects of the CP nanocrystals were observed in the PB nanoparticles. It is noteworthy that the magnetic properties of the PB nanocrystals including nanoparticles and nanowires showed different features compared with the bulk materials. The magnetic breaking temperatures (T_c) of the nanocrystals where the PB analogues turn to ferromagnetic compounds were reported to be often lower than those of corresponding bulk materials.^{11,12,14} In addition, the PB analogue nanoparticles were found to show superparamagnetic behaviors due to the single magnetic domain in one particle.^{9,11b,12} These magnetic behaviors arise from the drastic decrease in the grain size and the increase in the surface-to-volume ratio of the PB nanoparticles. Especially, in the studies of the polymer-protected PB nanoparticles, it was observed that T_c depends on the particles size (Figure 9).¹¹ Moreover, the magnetic properties of PB nanoparticles are affected by the surface protected polymer.^{11b} One polymer (PDDA) on the surface of the PB nanoparticles enhances the magnetic coupling in PB compared to another polymer (PVP) protection system. On the other hand, the absorption spectra of the PB nanoparticles protected by the organic polymers showed apparent shifts of intermetal charge-transfer (CT) band from Fe^{2+} to Fe^{3+} compared with that of bulk PB because of large area interactions between the surface polymers and the inner PB particles. The absorption maxima for CT bands of the PB nanoparticles with the different polymer protections showed different absorption shifts (Figure 10).^{11b} This fact indicates that the surface-protecting polymers give a great influence on the energy expended in trans-

ferring the electron from Fe^{II} to Fe^{III} in the PB nanoparticles, resulting in the changes in their magnetic property. Moreover some PB nanoparticles showed a solvent-dependent CT absorption due to the change at the surface environment.

Higher ordered structures and film formations can be achieved by the CP nanocrystals covered with long alkyl ligands or polymers. In the studies of AOT-protected PB analogue nanoparticles, they assembled into nanoparticle array with superlattice ordering by the highly hydrophobic surface of the PB nanoparticles (Figure 4).⁸ The superlattice structures were organized with 60–100 nanoparticles while the individual nanoparticles were separated by 2–3 nm spacing, which is consistent with an interdigitated bilayer of AOT. Similar superlattice structure was observed in the study of the stearylamine protected PB analogue nanoparticles.¹⁰ The surface polymer protections not only enhance solubilities of the PB nanoparticles in organic solvents but also provide film-forming properties when the colloidal dispersions of the composites are evaporated,¹¹ suggesting a technological advantage toward processable CP materials.

Transformation of the CP nanocrystals into different nanomaterials with ordered morphologies is an attractive subject. In case of the CP crystals [$\text{ZnF}(\text{AmTAZ})$], the submicron rodlike CP crystals could be transformed to inorganic rod-crystals with the shape retained.¹⁶ Calcination of the CP crystals at elevated temperature under O_2 and N_2 produced wire crystals of ZnO and ZnCN_2 , respectively, suggesting possible route for preparation of one-dimensional inorganic nanomaterials by use of CP precursors (Figure 11).

◆ Summary and Perspectives

This review illustrates an early but evolving stage of the studies on syntheses and some properties of the CP nanocrystals and the related compounds. In the current situation, most of the research efforts have devoted to the syntheses of the CP nanocrystals, and their nanosize effects have been explored. In the studies of the PB nanoparticles, it turns out that the particle sizes and the surface environments affect both the optical and magnetic properties. These studies would give valuable information for future applications of the PB analogues to nanomagnetic materials that attract growing interest because of their potential in ultrahigh-density magnetic recording systems.¹⁹

As we described in this review article, the syntheses of CP nanocrystals with organic ligands have not been achieved yet. Such organic–inorganic nanocrystals with a variety of combinations may be utilized in the development of advanced nanomaterials because of weak bonding interaction and versatility of the electronic state. Considering those, the advantageous features of “CP nanocrystals” are expected as follows (Figure 12).

- 1. Chiral nanocrystals;** Nanocrystals of CP with chiral ligand will show some advanced properties. One can realize that the CP nanocrystals with chiral bridging ligands and active transition metals may be used as intelligent catalysts in asymmetric reactions. Another advantage of the chiral CP nanocrystals is capability for constructions of complicated nanostructures such as twists, helices, and spirals.
- 2. Porous nanocrystals;** In the research area of the bulk CP materials, porous CP is now center of interest for their zeolitic applications. If the porous CP crystals can be deduced into nanometer scale with precise size and shape controls,

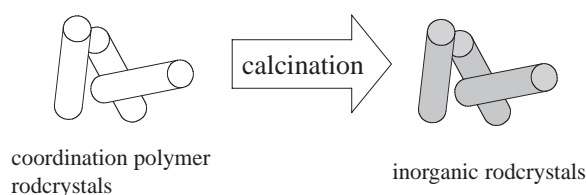


Figure 11. Transformation of CP crystals to inorganic materials with the one-dimensionality retained.

the resultant nanosize crystals will not only show the improved zeolitic functions but also open new nanoscience of the porous materials. The attractive and potential matters for such materials are unprecedented adsorption, precise guest inclusion, pore orientation, and nanofluidics. For example, the porous CP nanocrystals may be applied to guest molecular carriers and drug delivery systems (DDS). Depending on the crystals size, the porous CP crystals can control the number of the incorporated guest molecules in the pores, which will lead to a molecular-weight-controlled polymerization system when organic monomers are employed as the guest molecules. Such attempts are now undertaken by our group.

3. **Soft nanocrystals;** Responding to external physical or chemical stimuli, the noncovalent bonded CP structures often exhibit soft and dynamic behaviors. It is difficult for the rigid inorganic nanomaterials to achieve the flexible conformational changes. Work on the CP nanocrystals with dynamic structures, which can be manipulated by heat, light, redox, spin transitions, and host-guest interaction, should be interesting. For example, the accessible and movable electrons in the metal complexes lead to drastic phase transition behaviors based on the different electronic states. Therefore CP nanocrystals with the dynamic structures may be applied to sensors, memories, indicating materials, nanoreactors, and nanoactuators, which can open another scope in nanomaterials science.

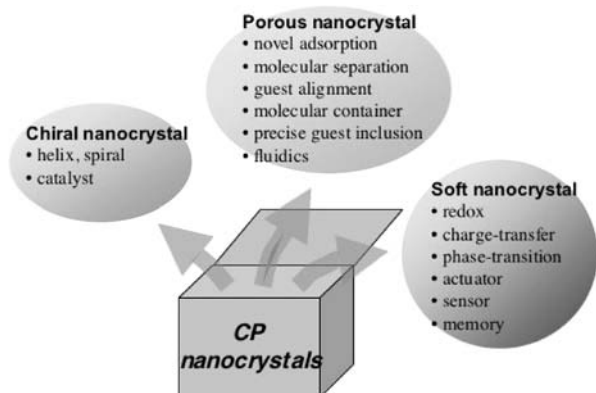


Figure 12. Expected properties of CP nanocrystals.

The research of the CP nanocrystals is just one topic in the subjects focusing on the crystal size and morphology of CP. Study on crystal growth controls of CP with requisite sizes from mm to nm regime and desired morphologies from 0-dimensional to more complicated shapes, which is still in its infancy, should find new features different from inorganic materials and contribute to the development of the CP chemistry. We will witness the beginning of what science develops between the research areas of coordination chemistry and materials chemistry.

References

- a) "Clusters and Colloids," ed. by G. Schmid, VCH, Weinheim (1994). b) A. P. Alivisatos, *Science*, **271**, 933 (1996). c) P. V. Kamat, *J. Phys. Chem. B*, **106**, 7729 (2002). d) J. Hu, T. Odom, and C. M. Lieber, *Acc. Chem. Res.*, **32**, 435 (1999). e) X. Duan, Y. Huang, Y. Cui, J. Wang, and C. M. Lieber, *Nature*, **409**, 66 (2001).

- a) H.-B. Fu and J.-N. Yao, *J. Am. Chem. Soc.*, **123**, 1434 (2001). b) F. Debuigne, L. Jeuniau, M. Wiame, and J. B. Nagy, *Langmuir*, **16**, 7605 (2000). c) S. Takahashi, H. Miura, H. Kasai, S. Okada, H. Oikawa, and H. Nakanishi, *J. Am. Chem. Soc.*, **124**, 10944 (2002). d) H. Kasai, H. Kamatani, S. Okada, H. Oikawa, H. Matsuda, and H. Nakanishi, *Jpn. J. Appl. Phys.*, **34**, L221 (1996). e) N. D. Denkov, O. D. Velev, P. A. Kralchevsky, I. B. Ivanov, H. Yoshimura, and K. Nagayama, *Nature*, **361**, 26 (1993). f) E. Adachi, A. S. Dimitrov, and K. Nagayama, *Langmuir*, **11**, 1057 (1995). g) Y. Chen, W. T. Ford, N. F. Materer, and D. Teeters, *Chem. Mater.*, **13**, 2697 (2001). h) D. T. Bong, T. D. Clark, J. R. Granja, and M. R. Ghadiri, *Angew. Chem., Int. Ed.*, **40**, 988 (2001). i) A. Harada, J. Li, and M. Kamachi, *Nature*, **356**, 325 (1992). j) H. Furusawa, A. Fukagawa, Y. Ikeda, J. Araki, K. Ito, G. John, and T. Shimizu, *Angew. Chem., Int. Ed.*, **42**, 72 (2003).
- B. Moulton and M. J. Zaworotko, *Chem. Rev.*, **101**, 1629 (2001).
- a) S. Kitagawa, R. Kitaura, and S. Noro, *Angew. Chem., Int. Ed.*, **43**, 2334 (2004). b) C. Janiak, *Dalton Trans.*, **2003**, 2781.
- a) N. Kimizuka, *Adv. Mater.*, **12**, 1461 (2000). b) C. Mingotaud, C. Lafuente, J. Amiell, and P. Delhaes, *Langmuir*, **15**, 289 (1999). c) Y. Einaga, O. Sato, T. Iyoda, A. Fujishima, and K. Hashimoto, *J. Am. Chem. Soc.*, **121**, 3745 (1999).
- a) F. E. Kruijs, H. Fissan, and A. Peled, *J. Aerosol. Sci.*, **29**, 511 (1998). b) D. B. Geohegan, A. A. Puretzky, G. Duscher, and S. J. Pennycook, *Appl. Phys. Lett.*, **72**, 2987 (1998). c) D. V. Goia and E. Matijevic, *New J. Chem.*, **22**, 1203 (1998). d) H. Bonnemant and R. M. Richards, *Eur. J. Inorg. Chem.*, **2001**, 2445. e) P. S. Shah, S. Husain, K. P. Johnston, and B. A. Korgel, *J. Phys. Chem. B*, **105**, 9443 (2001). f) J. C. Hulteen and C. R. Martin, *J. Mater. Chem.*, **7**, 1075 (1997). g) A. Huczko, *Appl. Phys. A*, **70**, 365 (2000).
- a) S. Ohkoshi, Y. Abe, A. Fujishima, and K. Hashimoto, *Phys. Rev. Lett.*, **82**, 1285 (1999). b) S. Ferlay, T. Mallah, R. Quahés, P. Veillet, and M. Verdager, *Nature*, **378**, 701 (1995). c) S. Ohkoshi, T. Iyoda, A. Fujishima, and K. Hashimoto, *Phys. Rev. B*, **56**, 11642 (1997). d) S. Ohkoshi, S. Yoroze, O. Sato, T. Iyoda, A. Fujishima, and K. Hashimoto, *Appl. Phys. Lett.*, **70**, 1040 (1997). e) O. Sato, T. Iyoda, A. Fujishima, and K. Hashimoto, *Science*, **272**, 704 (1996).
- a) S. Vaucher, M. Li, and S. Mann, *Angew. Chem., Int. Ed.*, **39**, 1793 (2000). b) S. Vaucher, J. Fielden, M. Li, E. Dujardin, and S. Mann, *Nano Lett.*, **2**, 225 (2002).
- L. Catala, T. Gacoin, J.-P. Boilot, E. Riviere, C. Paulsen, E. Lhotel, and T. Mallah, *Adv. Mater.*, **15**, 826 (2003).
- M. Yamada-Sasano, M. Arai, M. Kurihara, M. Sakamoto, and M. Miyake, *J. Am. Chem. Soc.*, **126**, 9482 (2004).
- a) T. Uemura and S. Kitagawa, *J. Am. Chem. Soc.*, **125**, 7814 (2003). b) T. Uemura, M. Ohba, and S. Kitagawa, *Inorg. Chem.*, **43**, 7339 (2004).
- J. G. Moore, E. J. Lochner, C. Ramsey, N. S. Dalal, and A. E. Stiegman, *Angew. Chem., Int. Ed.*, **42**, 2741 (2003).
- J. M. Dominguez-Vera and E. Colacio, *Inorg. Chem.*, **42**, 6983 (2003).
- P. Zhou, D. Xue, H. Luo, and X. Chen, *Nano Lett.*, **2**, 845 (2002).
- L. Huang, H. Wang, J. Chen, Z. Wang, J. Sun, D. Zhao, and Y. Yan, *Microporous Mesoporous Mater.*, **58**, 105 (2003).
- L. Guo, C. Liu, R. Wang, H. Xu, Z. Wu, and S. Yang, *J. Am. Chem. Soc.*, **126**, 4530 (2004).
- C.-Y. Su, A. M. Goforth, M. D. Smith, P. J. Pellechia, and H.-C. zur Loye, *J. Am. Chem. Soc.*, **126**, 3576 (2004).
- S. A. Davis, M. Breulmann, K. H. Rhodes, B. Zhang, and S. Mann, *Chem. Mater.*, **13**, 3218 (2001).
- a) C. T. Black, C. B. Murray, R. L. Sandstrom, and S. Sun, *Science*, **290**, 1131 (2000). b) S. Sun, C. B. Murray, D. Weller, L. Folks, and A. Moser, *Science*, **287**, 1989 (2000). c) S. Hashimoto, A. Maesaka, K. Fujimoto, and K. Bessho, *J. Magn. Mater.*, **121**, 471 (1993).